CATRINA (2024), 31 (1):-87-98

Protective Effects of *Turbo cornutus* Extract Against $HgCl_2$-Induced Pathological Changes in Albino Rat Tissues

Yasmin M. Abd El-Aziz*, Merna M. Kazlak, Nada H. Farouk, Mariam M. Helmy, Aya R. Mohamed, Nora M. Awad, Rana Y. Hamed, Ali H. Abu-Almaaty
Zoology Department, Faculty of Science, Port Said University, Port Said, 42526, Egypt.

Received: April 30, 2024; Accepted: July 16, 2024

ABSTRACT

Mercuric chloride ($HgCl_2$) is a highly toxic form of mercury and a harmful environmental pollutant. This study investigated the protective effects of *Turbo cornutus* visceral extract against the damaging impacts of $HgCl_2$ exposure on growth rate, blood parameters, and histopathological changes in various organs of rats. *Turbo cornutus* is a sea snail species whose visceral extract is composed of a variety of antioxidants and could be easily available for the treatment of the harmful effects induced by mercuric chloride. In this study, 40 male rats were randomly divided into 4 groups (10 rats per 2 cages): control group (G1), group ingested with 200 mg/kg of *T. cornutus* visceral extract (G2), group exposed to 1/20 of the LD_{50} dose of $HgCl_2$ (G3), and the last group was toxic plus treatment group (G4) receiving the same doses as G2 and G3. After 5 weeks of feeding, the rats were euthanized, and the results were recorded. The *T. cornutus*-treated rats (group 2) showed stable measurements compared to the control group (G1). Exposure to $HgCl_2$ resulted in alterations in growth rate, blood parameters, and histopathological changes, including Kupffer cell enlargement in the liver, renal tubular damage, and heart edema. However, the administration of *Turbo cornutus* visceral extract reduced the $HgCl_2$-induced damage and preserved the integrity of the organs. The obtained results demonstrate the protective effects of *Turbo cornutus* visceral extract against $HgCl_2$-induced toxicity in rats. The antioxidant properties of the extract may contribute to its ability to mitigate the harmful effects of mercuric chloride exposure. Further studies are needed to elucidate the underlying mechanisms and explore the potential therapeutic applications of *T. cornutus* visceral extract in heavy metal toxicity management.

Key words: Chromosomes; Histochemistry; Histopathology; Mercuric chloride; Protective effect; *Turbo cornutus*.

INTRODUCTION

Mercury is a potent environmental pollutant that poses significant risks to human health and wildlife. Exposure to mercury, particularly in its inorganic form such as mercuric chloride ($HgCl_2$), can lead to severe pathological changes in various tissues, including the liver, kidneys, and brain. These changes are often characterized by oxidative stress, inflammation, and cellular damage, ultimately resulting in compromised organ function and increased morbidity. As a result, there is a growing interest in identifying natural compounds that can mitigate the harmful effects of mercury exposure (Oriquat *et al*., 2012). Human body accumulates the in-taken amounts of mercury in r kidney, liver, and other tissues, mercury and its compounds have the toxic scope of changing the nature of biological proteins, enzymes, and the uptake and release of neurotransmitters (Ezeuko *et al*., 2007).

The degree of mercury toxicity depends on its type and chemical formula, mercuric chloride is a mercury salt type, and it is found in a very poisonous form. It has strong acute toxic effects and produces nephritis, which affects the nervous system, besides gastrointestinal dysfunction (Huang *et al*., 1996). $HgCl_2$ forms organomercury complexes with proteins. Once mercuric chloride is bound to the glutathione (GSH), the Hg leaves the cell to circulate in lymph and is deposited in other organs, there have been a lot of studies in both humans and animals on the impacts of mercuric chloride in the renal system, liver, and cardiovascular system (Boujbiha *et al*., 2009).

Human exposure to mercury primarily occurs through the consumption of contaminated fish and seafood, inhalation of mercury vapors, and dermal contact with mercury-containing products. The effects of mercuric pollution on the human body can be profound and varied, impacting multiple organ systems. Acute exposure can lead to neurological and cognitive impairments, while chronic exposure is associated with serious health issues, including kidney damage, respiratory problems, and developmental disorders in children. In addition, mercuric chloride ($HgCl_2$) has been shown to induce significant genotoxic effects in rats, affecting their chromosomes. Moreover, exposure to mercuric chloride can lead to DNA damage in various cells, including leukocytes. This damage manifests as chromosomal aberrations, which are indicators of genotoxicity and can lead to various health issues in the affected organisms (Paramjit *et al*., 2001). Understanding the sources and effects of mercuric pollution is essential for developing effective strategies to mitigate its impact on public health and the environment.

* *Corresponding author e-mail: **yasminabdelaziz2012@yahoo.com***

Turbo cornutus, commonly known as the horned turban sea snail or Japanese turban shell, is a marine gastropod mollusk found along the southern coast of Korea, particularly on Jeju Island. The main habitats of *Turbo cornutus* are the rocky intertidal zone and shallow subtidal areas at depths up to 20 meters, hallow subtidal areas at depths up to 20 meters, beds of articulated coralline algae and rocky habitats with water temperatures ranging from 20 to 25°C, occurring along the Kuroshio Current in the northwestern Pacific Ocean (Kim *et al*., 2022). In Egypt, this sea snail inhabits regions rocky intertidal zones, coralline algae beds and shallow subtidal areas that offer hard substrates and abundant algae, making these environments crucial for its survival and ecological role in the marine ecosystem.

Turbo cornutus has several important aspects for human health and the ecosystem. Among its importance are their nutritional values where *T. cornutus* is a good source of protein, lipids, and various nutrients. It contains high levels of beneficial fatty acids like arachidonic acid and n-3 docosapentaenoic acid (Kim *et al*., 2022). *T. cornutus* also has potential health benefits, where extracts from *T. cornutus* viscera have demonstrated antioxidant effects against hydrogen peroxide-induced oxidative stress in cells by regulating MAPK and Akt signaling pathways. The ethanolic extract of *T. cornutus* viscera also exhibits anti-inflammatory properties (Kim *et al*., 2022; Saito and Aono, 2014).). Meanwhile, it possess bioactive peptides that may have important roles in promoting anti-inflammatory mechanisms and protecting different cell types.

Mitigating the effects of mercuric toxicity involves a combination of prevention, treatment, and public health strategies. Among the treatment that can be active and ecofriendly is using *T. cornutus* extracts. Therefore our study was designed to investigate the protective effects of *Turbo cornutus* visceral extract (TCVE) against pathological changes induced by mercury chloride ($HgCl_2$) in albino rat tissues. This includes assessing various biological parameters such as growth rate, chromosomal integrity, hematology, physiological parameters, and histopathological changes that occurred in liver, kidney and heart, in the treated rats. By evaluating the chromosomal and histopathological alterations in response to mercury exposure and subsequent treatment with *T. cornutus* extract, elucidation the potential of this marine mollusk as a natural therapeutic agent could contribute to the development of novel strategies for mitigating the adverse effects of mercury toxicity, thereby enhancing both environmental and public health.

MATERIALS AND METHODS

Ethical approval

This study was conducted in accordance with the ethical procedures and policies established by the Animal Care Committee at the Faculty of Science, Port Said University, Port Said, Egypt (ERN: PSU.Sci.41).

Chemical used: dosage and delivery Methods

Mercury(II) chloride ($HgCl_2$), used in this study as a toxic agent, was purchased from Sigma-Aldrich. The lethal dose 50 (LD_{50}) of $HgCl_2$ was 75 mg/kg (Oriquat *et al*., 2012). It was administered to rats in equal doses in G3 and G4 cages (toxic and toxic plus treatment), dissolved in saline solution (1:1 for W/V), and given orally through the drinking water of the rats twice weekly.

Turbo cornutus visceral extract (TCVE)

The *T. cornutus snail* was obtained from a seafood market in Port Said, Egypt. The first step involved washing its surface with distilled water and removing the viscera. Afterward, the viscera were washed again with distilled water, dried, and ground into a powder using a grinding machine. The powder was then dissolved in methanol (1:4 for W/V) for one day, followed by filtration, which was performed three times. The resulting mixture was placed in a rotary evaporator at a temperature of 60°C, yielding a concentrated extract. This extract was stored in glass vials at -15°C for future use. The preparation method was based on the protocols established by Cunha *et al*. (2004) and Abu Almaaty *et al*. (2022).

Experimental design

This study was performed at the animal house in the Faculty of Science, Port Said University. Forty male albino rats (117-120 g) were obtained from the veterinary animal center in Helwan City and randomly classified into 4 groups, with each cage containing 10 rats (Figure 1). G1 served as the control group. G2 received a treatment dose of 200 mg/kg of *T. cornutus* viscera extract (TCVE) (Abu Almaaty *et al*., 2022). G3 received a mercuric chloride dose of 1/20 of the LD50 (Oriquat *et al*., 2012). G4 received both the toxic dose from G3 and the treatment dose from G2.

All groups had access to drinking water, regular nutrients, and growth supplements in their diet. G2 and G4 received their treatment dose three times weekly, while G3 and G4 received their toxic dose twice weekly. All cages were provided with a regular diet. The experimental rats were maintained under ideal constant environmental conditions, including a temperature of 25±3°C, humidity of 45±3%, and a suitable light-dark cycle. They were housed in plastic cages.

This study was conducted for a period of 5 weeks. Blood samples were collected in plastic tubes containing anticoagulant. Subsequently, tissue proce-ssing was performed on the kidneys, liver, and heart for histopathological and histochemical examinations.

Measurement parameters

Growth rate

In this experiment, the body weight of each rat was measured daily, three times per week. Body weight gain was calculated using the following equation:

$$Growth\ rate = \frac{Weight_{\ current\ week} - Weight_{\ pervious\ week}}{Weight_{\ pervious\ week}}$$

This calculation was performed for each group of rats (n=10).

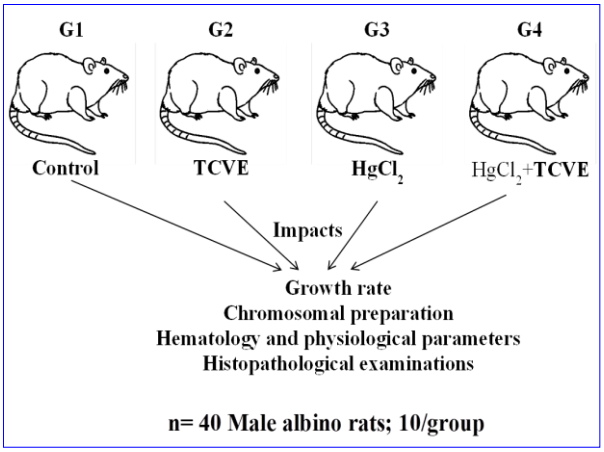

Figure (1): Experimental design showing different treatment groups and the measured parameters.

Chromosomal preparation

After 5 weeks, the rats were fasted for one day. Five rats from each group were injected intraperitoneally with 0.5 ml of 1% colchicine one hour before sacrifice to prepare for chromosomal examinations. Bone marrow samples were then collected from the rats' bones and processed using the method described by Singh and Sankhla (2010). The chromosomal slides were stained with Giemsa stain and subsequently examined under an optical microscope.

Blood chemistry

An additional five rats in this study were euthanized, and blood samples were collected from them (n=5 for each group) in tubes containing anticoagulant. The samples were mixed thoroughly to ensure homogenyization and then centrifuged at 3000 rpm for 20 mins.

The obtained plasma was analyzed using a spectrophotometer. Lactate dehydrogenase (LDH) activity was evaluated according to the method described by King and Weber (1986). Creatinine kinase (CK) activity was determined following the protocols established by Francis *et al*. (2023) and Norman *et al*. (1977). Glucose levels were assessed based on the method outlined by McMillin (1990). Total protein concentration was determined following the method of Waterborg (2009). The assay kits were obtained from Bio-Diagnostic (Giza City, Egypt).

Histopathological and histochemical examinations

Samples of the liver, kidneys, and heart were removed, washed with saline solution, then fixed with neutral formalin solution (10%), and passed through the tissue processing steps of dehydration, clearing, embedding, and making paraplast wax blocks. Then they are cut with a 5-micron thickness microtome device, then hematoxylin and eosin (H and E) stains for prepared tissues (Fischer *et al*., 2008), and Masson trichrome stain (MT) is used to visualize connective tissue and collagen in tissue sections, it is a special stain used for hepatic tissues and stains a red background against the blue color of collagen. Also, it is used to identify hepatic pathologies or kidney pathologies (Almatrafi, 2024; Krishna, 2013), finally examined under a light microscope.

Statistical analysis

Statistical analysis was conducted on the data obtained, which are presented as the mean of three replicates ± standard error (SE). The significance of the results for the experimental rats was assessed using Tukey's test, with the following designations based on the level of significance: *** indicates a highly significant difference at $p \leq 0.001$; ** denotes a significant difference at $p \leq 0.05$. The analyses were carried out using the SPSS version 21 software.

RESULTS

Impact of *T. cornutus* Extract on Mercuric Chloride Toxicity

Growth rate

The results of weekly average gain weights (Figure 2), showed that the weight gain trends seem to differ across the groups, with some groups gaining more weight than others over the 5-week period. The G1 (control) had a decrease in weight at the 4th week (20 g). However, TCVE Group (G2) recorded an increase in weight across the time period of the experiment. For $HgCl_2$ Group (G3), a significant weight loss highlights the severe toxicity associated with mercuric chloride. The weight drop from 25 g to less than 5 g indicates a critical impact on the rats' health. However, G4 recoded a mixed results in which recovery in weight gain was observed by 4th and 5th week of the experiment. This may indicate a complex interaction between $HgCl_2$ and TCVE. This may reflect the mitigation effect of TCVE against the toxicity of $HgCl_2$.

Chromosomal examinations

The genotoxicity induced by mercuric chloride on chromosomal aberrations was examined in comparison to the control groups G1 and G2. For the control groups G1 and G2, normal chromosomal appearance without any alterations was recorded (Figure 3A-B). In contrast, for group G3 ($HgCl_2$), chromosomal abnormalities were observed, including ring chromosomes, deletions, breaks, and fragmentation of chromosomes (Figures 4A-B). Meanwhile, for group G4 ($HgCl_2$+TCVE), the appearance of the chromosomes was better preserved compared to G3, showing a decrease in the incidence of deletions, breaks, and fragments (Figure 5A-B).

Evaluation of the blood biochemistry

The evaluation of biochemistry parameters measured in different groups was represented in Figure (6). LDH value was significantly increased in the blood plasma of rats intoxicated with mercuric chloride compared to the control group (G1). In addition, treatment with TCVE in G4 ($HgCl_2$+TCVE) showed reduction in LDH levels compared to G3 in which treated only with $HgCl_2$. The enzymatic activity of LDH significantly increased from 125.29±0.41 U/L in the control group (G1) to 134.71±2.22 U/L in the $HgCl_2$ group (G3). However, the TCVE group (G2) maintained at normal levels of 125.28±0.52 U/L. In contrast, the G4 showed

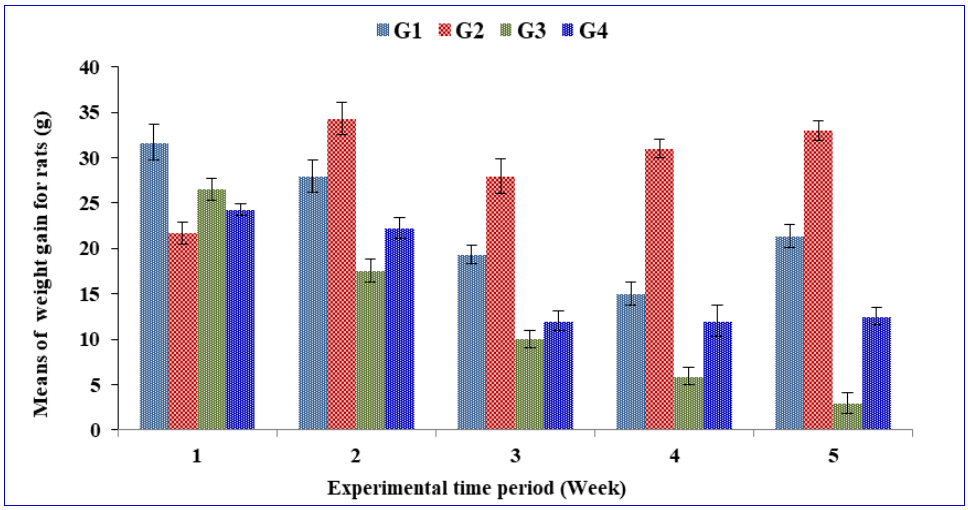

Figure (2): Impact of *T. cornutus* extract on mercuric chloride toxicity of different experimental group showing the growth rate, mean±SE, represented by weight gain across five week periods. G1, control group; G2, rats administrated TCVE; G3, rats treated with $HgCl_2$, and G4, rats treated with a mixture of $HgCl_2$ and TCVE.

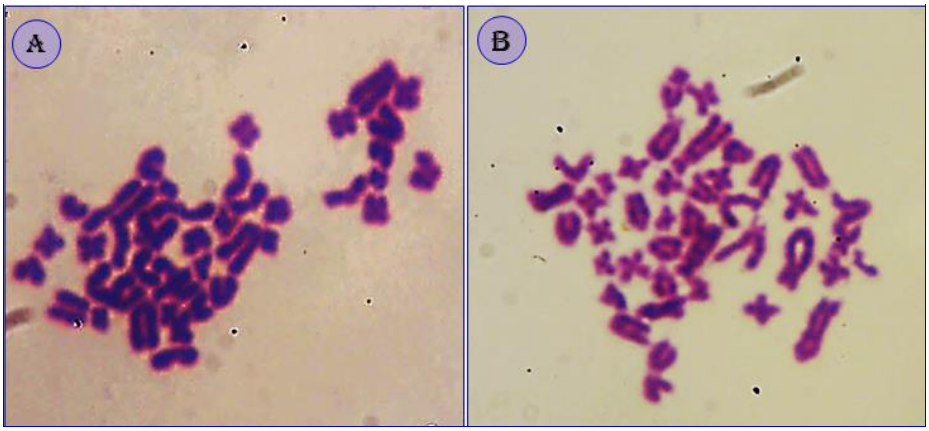

Figure (3): Normal chromosomes (42n) of Albino rats in control and TCVE groups (G1 and G2, respectively A, control group (G1); B, group received TCVE (G2). Gemisa stain, 1500X.

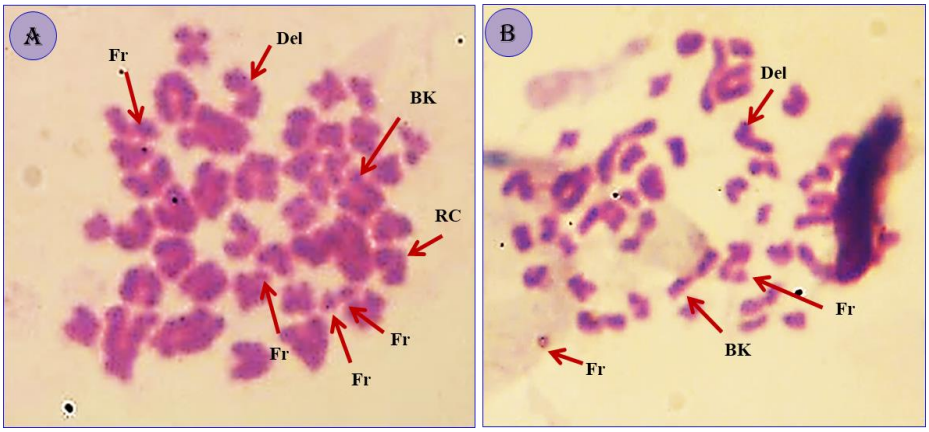

Figure (4): Chromosomal aberrations in Albino rats in G3 showing different abnormalities. Del; deletion, BK, break; RC, ring chromosome; and Fr: fragments Gemisa stain, 1500X.

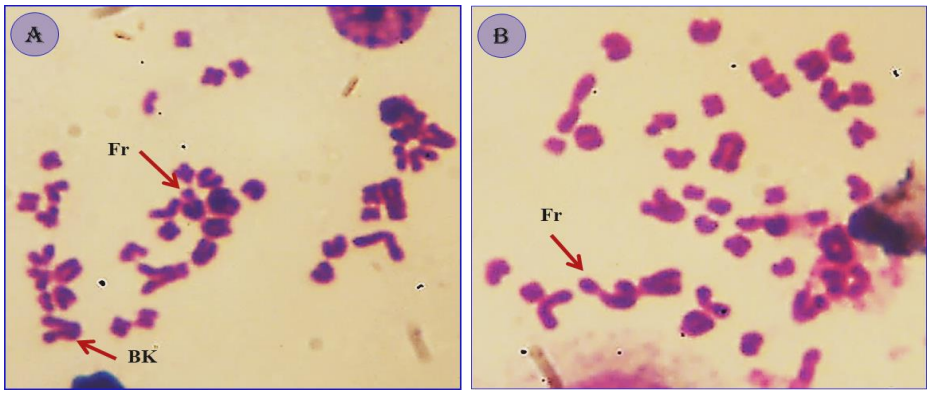

Figure (5): Chromosomal aberrations in Albino rats in G4 showing different abnormalities with less abundance. A, showing chromosomal break (BK) and fragments (Fr). B, chromosomal fragment (Fr) is seen. Gemisa stain, 1500X.

moderate reduction in LDH value (130.1944± 1.79) compared to G3 (134.71±2.22 U/L) (Figure 6A).

The creatine kinase (CK) levels were significantly increased in the blood plasma of intoxicated rats. In contrast, the TCVE-treated group (G2) exhibited full protection, with CK values returning to normal levels similar to those of the control group (142.13±3.89 U/L for G2 and 153.41±4.95 U/L for G1). Conversely, group G3 recorded the highest CK value at 162.83±3.59 U/L compared to the other groups (Fig. 6B). Meanwhile, group G4 showed an increase in CK levels, but this was not significantly different from the normal range recorded in the control group (G1).

The detected total protein value, in experimental groups, showed variation among treated groups (Fig. 6C). The protein value detected in G3 treated with mercuric chloride, reported a significant decrease value (3.28±0.39 g/dL) compared to G1 (5.40±0.23 g/dL). For G2, (TCVE) protein value detected showed normal range as in G1 and no significant difference was recorded (5.58±0.23 and 5.40±0.23 g/dL, for G2 and G1, respectively). Meanwhile, G4 showed a decreased value of the total protein (4.12±0.33 g/dL) compared to G1 (5.40±0.23 g/dL).

In addition, the measured level of glucose, represented in Fig. (6D) was significantly increased in mercuric chloride-treated rats. The lowest glucose value was seen in G1 (control), while the highest glucose value was found in the $HgCl_2$-treated rats; the G2 group (TCVE) is in the normal value compared to the G1 group (control). The G4 group ($HgCl_2$+TCVE) shows a downward in the glucose value to the $HgCl_2$ group and an upward in the glucose value compared to the G1 (control). The value of glucose increased from 90.20±4.50 mg/dL in the G1 (control group) to 132.20±7.19 mg/dL in the $HgCl_2$ group (G3). The TCVE group (G2) showed a value of 91.00± 4.16 mg/dL and the $HgCl_2$+TCVE group (G4) showed a value of 127.00±4.75 mg/dL decreased than the rate of the $HgCl_2$ group (G3).

Histopathological examinations

The liver tissues were stained with hematoxylin and eosin (H&E) to evaluate the toxic effects $HgCl_2$ and the protective effects of *Turbo cornutus* (Fig. 7). Liver tissues from group G1 display healthy architecture, with normal cellular structures characterized by healthy

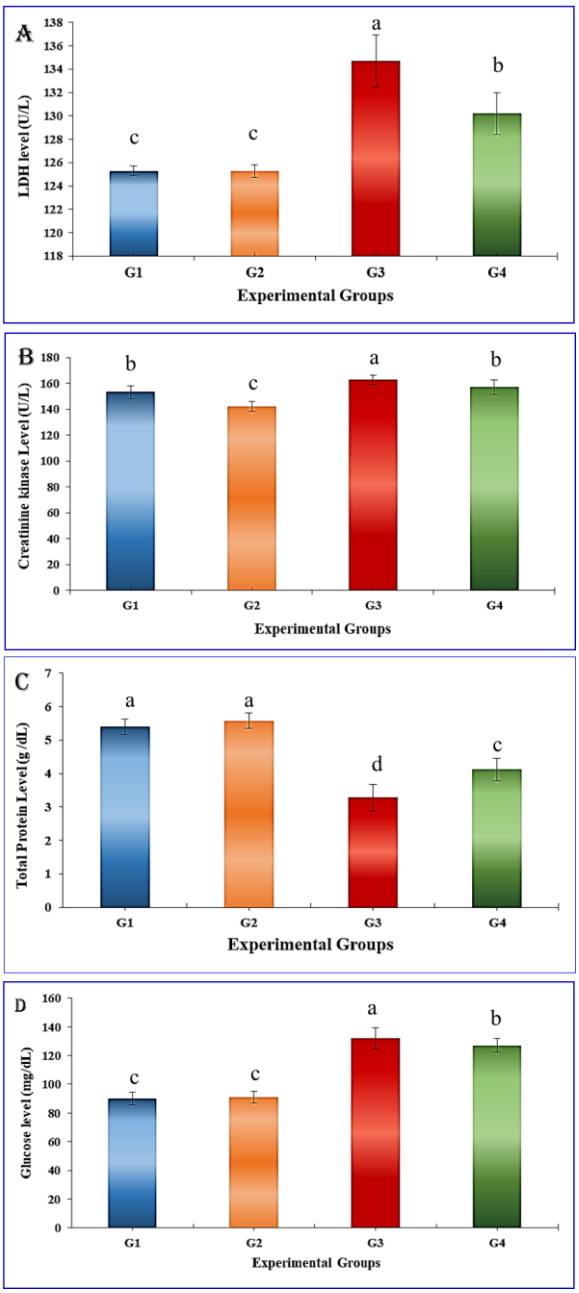

Figure (6): Blood biochemistry showing lactate dehydrogenase (LDH), Creatinine kinase (CK), total protein, and glucose levels in the four experimental groups. G1, control group; G2, TCVE; G3, HgCl2 and G4 group, HgCl2+TCVE. Columns with different letters are significantly different at $p \leq 0.05$

central veins and hepatic cells that have oval or rounded nuclei. The interstitial zones between liver strands contain numerous capillaries, known as liver sinusoids, which appear normal (Fig. 7A). The Kupffer cells are also observed to be normal. Group G2 exhibits a structure similar to that of group G1 (Fig. 7B). In contrast, the tissues of group G3, which were exposed to $HgCl_2$, show dilation of the central vein, enlargement of the sinusoidal spaces, and hypertrophy of the Kupffer cells (Fig. 7C). Meanwhile, the tissues from group G4 ($HgCl_2$ + TCVE-treated) recoded reduction in dilation of the central vein, narrower liver sinusoids, and healthier nuclei compared to the $HgCl_2$ group (Fig. 7D).

To explore the nature of connective tissues and collagen fibers, the Masson trichrome stain (MT) was employed. In groups G1 and G2, the normal architecture of the liver was observed (Fig. 8A-B). However, in group G3, treated with $HgCl_2$ (Figure 8C), dense fibrous septa, collagen fibers, and proliferation of the bile ducts were noted. In parallel, group G4 exhibited connective tissues and collagen fibers that were less dense and began to appear more normal (Figure 8D).

For kidney tissues, glomerulus with normal renal tubules and normal proximal tubules were observed (Figure 9A). In G2, the TCVE-treated tissues show a normal structure similar to the G1 (Figure 9B). However, the renal tissues exposed to $HgCl_2$ of the G3 showed degeneration of endothelium of some renal tubules and show some hyaline casts, a loss of nucleus, cells necrosis, and degeneration of glomerulus (Figure 9C). In contrast, G4 ($HgCl_2$ + TCVE-treated) showed less degeneration of glomerulus surrounded by bowman's capsule and less degeneration of the renal tubules (Fig. 9D).

$HgCl_2$ treatment resulted in significant deteri-oration of tubular cells, characterized by pyknotic nuclei and loss of nuclei, edema of the proximal tubules, atrophy of the glomeruli, and enlargement of Bowman's capsule, as demonstrated in the H&E-stained kidneys of $HgCl_2$-treated rats. Investigate the nature of the connective tissues and collagen fibers, using Masson trichrome (MT) stain, it was clear that G1 and G2, reflected normal architecture of the kidney (Figs. 10A-B). In contrast, group G3 exhibited a pattern of fibrous tissue formation within the glomeruli and in the interstitial tissue of the kidney (Fig. 10C). Markedly, an improvement in renal tissue and fibrous structures was observed in the $HgCl_2$ + TCVE-treated rats (G4, Fig. 10D).

For studying the histopathological elements of the myocardium, the G1 and G2 groups appear normal architecture of rats' myocardial, with normal muscle fibers branched with normal striation, normal nuclei, and normal intercalated disks (Figs. 11A-B). The G3 group shows degeneration of the branched muscle fibers, breakdown of striation and edema were found, and necrosis of nuclei also appeared within muscle fibers branched (Fig. 11C), the G4 shows little distortion of myofibers with improving striation, numerous normal nuclei are also present and detraction of the edema within muscle fibers (Fig. 11D).

For heart, with Masson's trichrome stain, groups G1 and G2 show the normal structure of cardiac muscle fibers (Figs. 12A-B), characterized by red staining of the healthy myocardium. In contrast, group G3 exhibits bright blue staining, indicating the presence of fibrotic tissue in the pericardium (Figure 12C). The fourth group (G4) shows a smaller amount of fibrosis and a less pronounced blue staining compared to the toxic group (G3), suggesting a lower degree of fibrotic

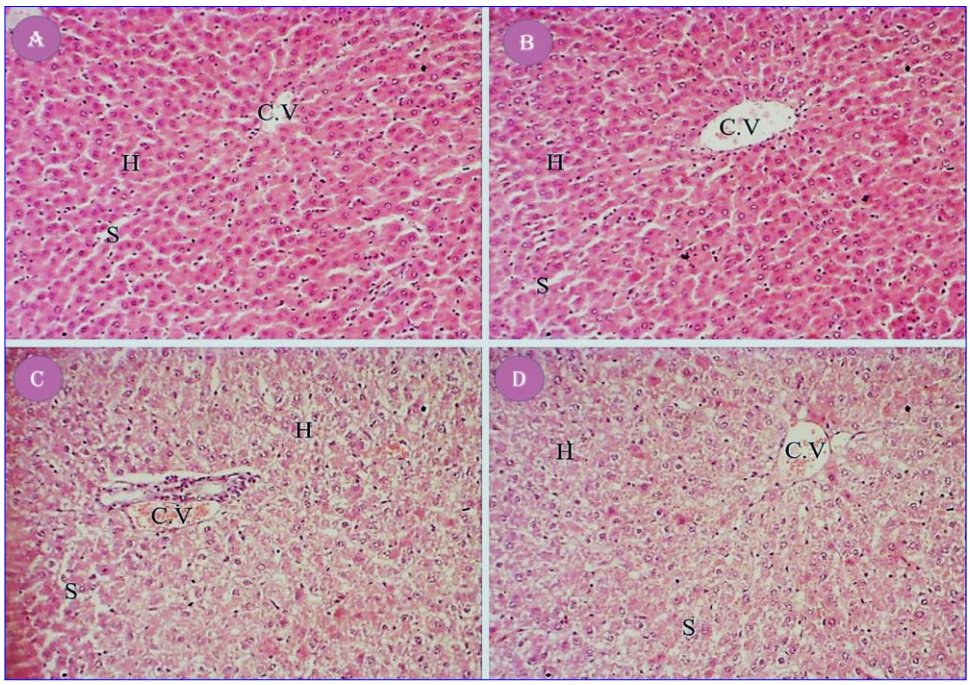

Figure (7): Hepatic tissue section photomicrographs of the four experimental groups showing C.V, central vein; H, hepatocytes and S, sinusoids. A, G1 (control); B, G2 (TCVE), C, G3 ($HgCl_2$) and D, G4 (HgCl2+TCVE). (H&E, 400X).

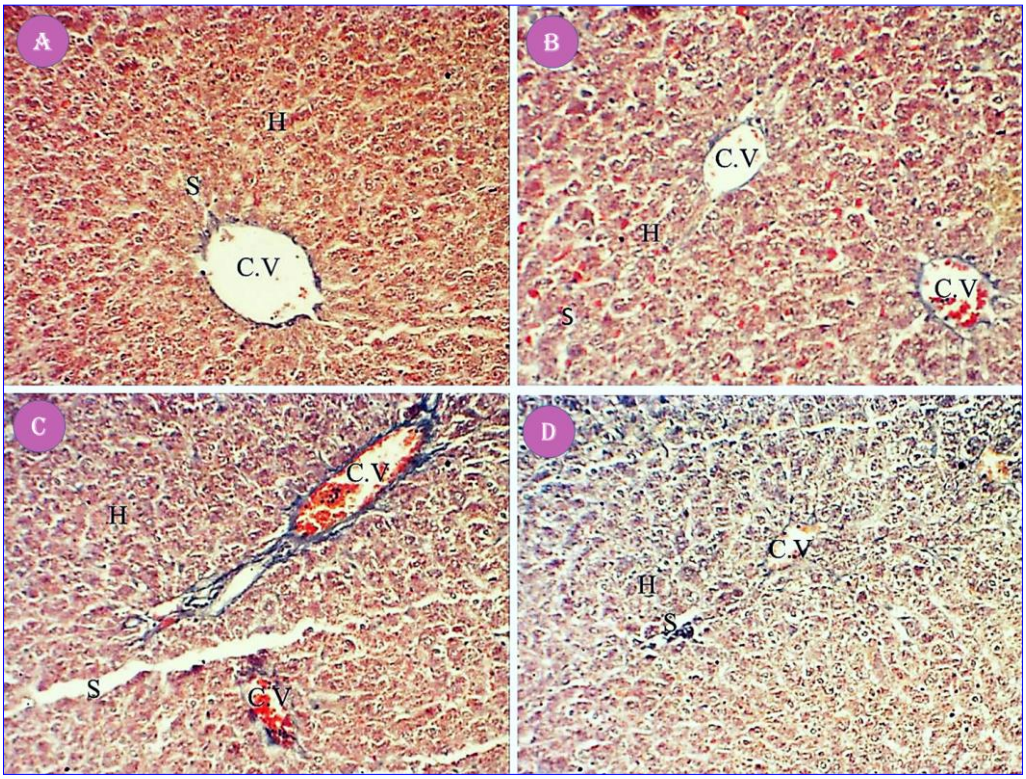

Figure (8): Hepatic tissue section photomicrographs of the four experimental groups showing C.V, central vein; H, hepatocytes and S, sinusoids. A, G1 (control); B, G2 (TCVE); C, G3 ($HgCl_2$) and D, G4 ($HgCl_2$+TCVE). (MT, 400X).

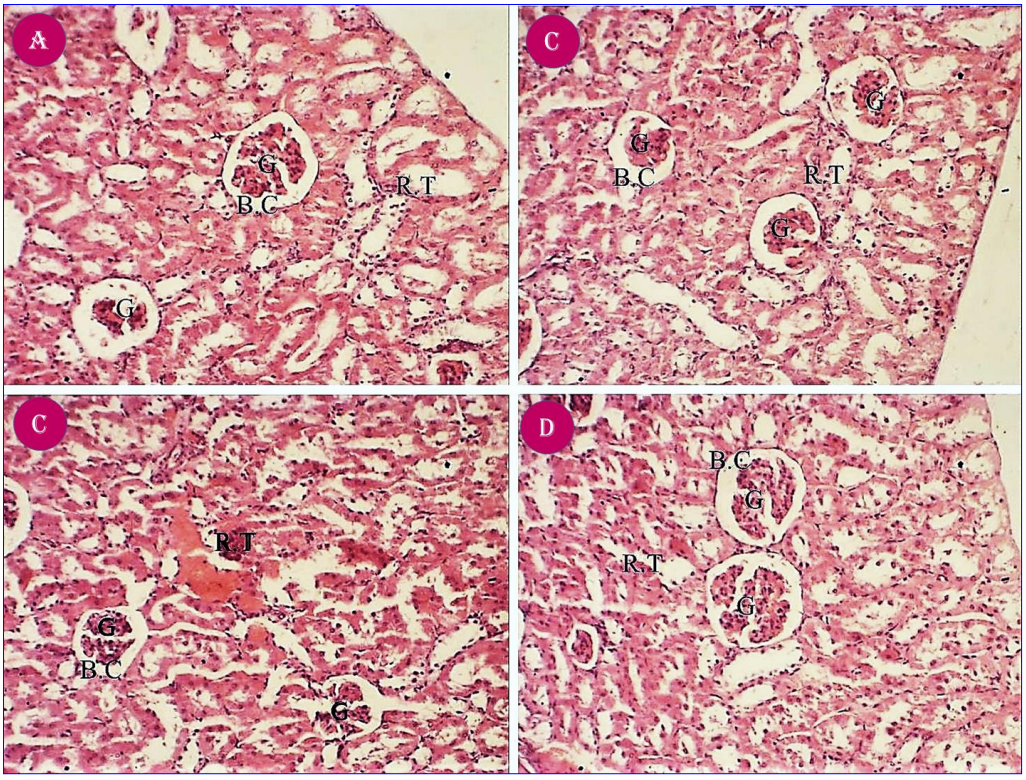

Figure (9): Renal tissues section photomicrographs of the four experimental groups showing B.C, Bowman's capsule; G, glomerulus, and R.T: renal tubules. A, G1 (control); B, G2 (TCVE); C, G3 ($HgCl_2$) and D, G4 ($HgCl_2$+TCVE). (H&E, 400X).

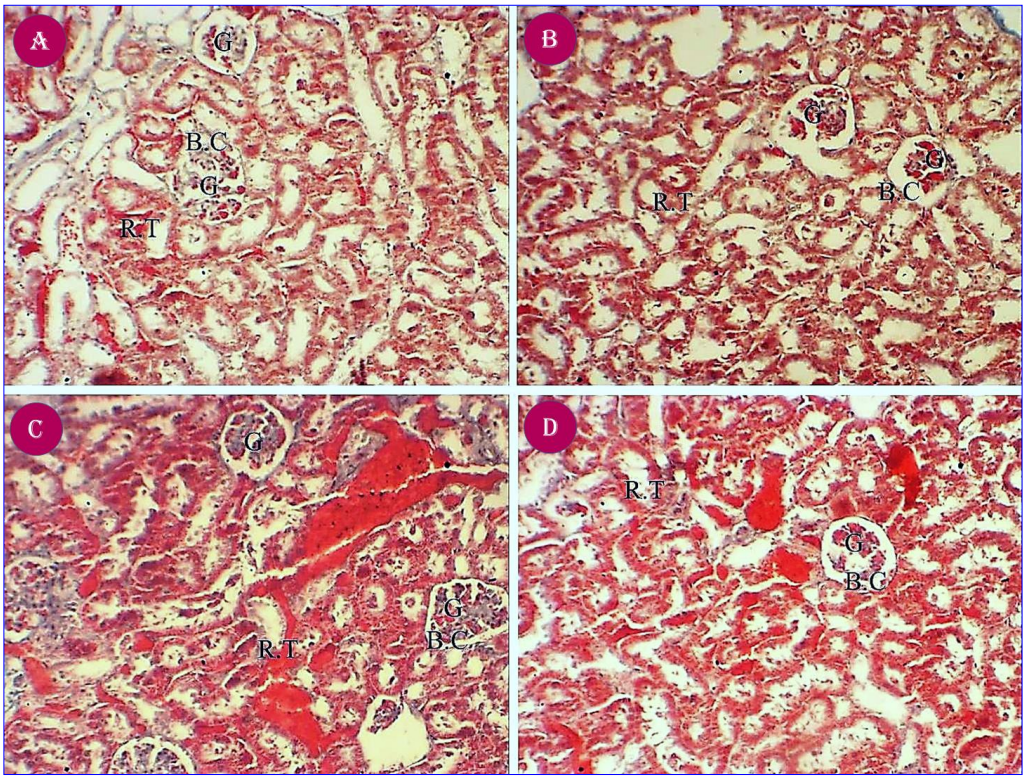

Figure (10): Renal tissues section photomicrographs of the four experimental groups showing B.C, Bowman's capsule; G, glomerulus and R.T, renal tubules. A, G1 (control); B, G2 (TCVE); C, G3 ($HgCl_2$) and D, G4 ($HgCl_2$+TCVE). (MT, 400X).

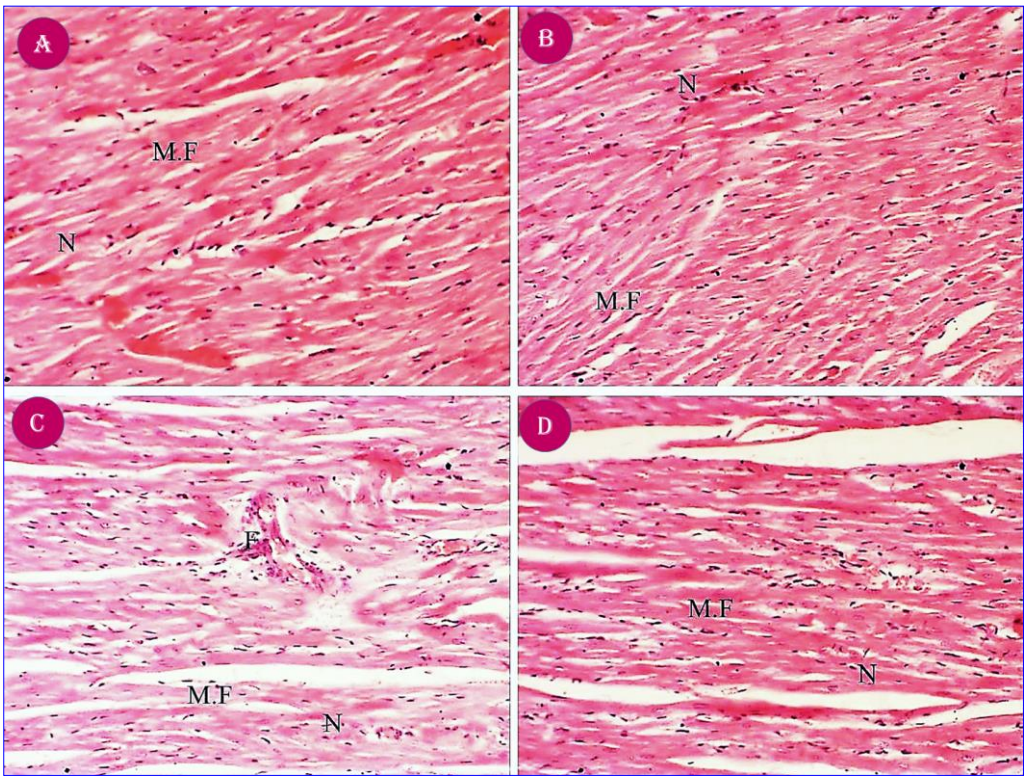

Figure (11): Myocardial tissue section photomicrographs of the four experimental groups showing M.F, muscle fibers; N, nuclei and F, inflammatory cells. A, G1 (control); B, G2 (TCVE); C, G3 ($HgCl_2$) and D, G4 ($HgCl_2$+TCVE). (H&E, 400X).

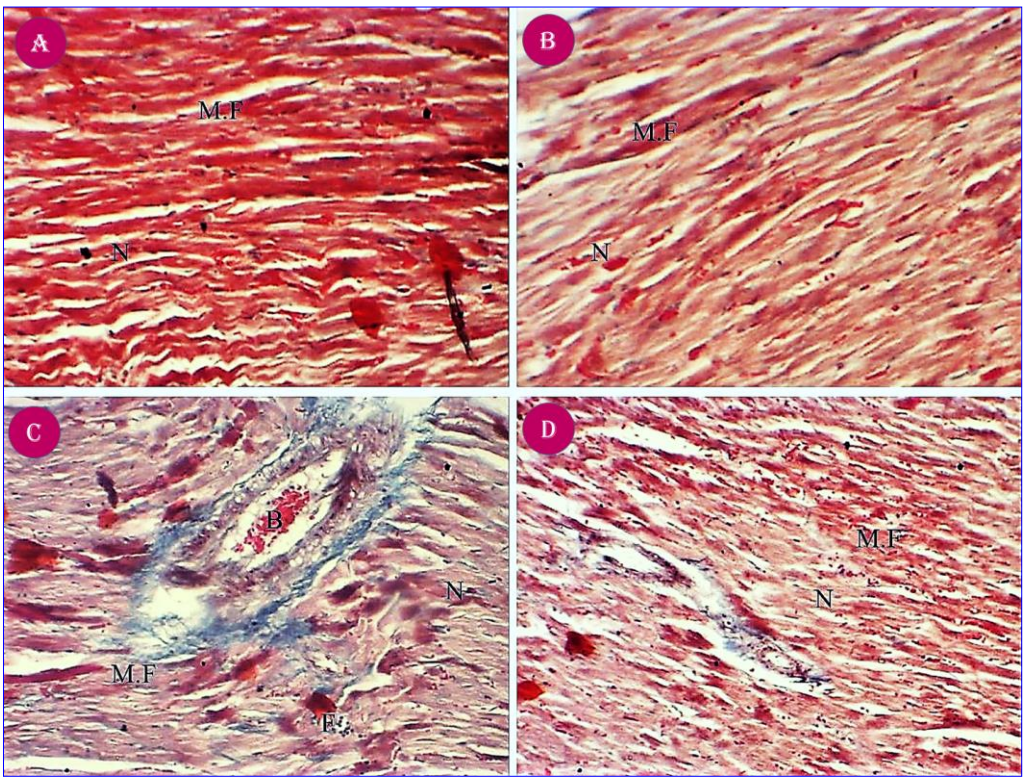

Figure (12): Myocardial tissue section photomicrographs of the four experimental groups showing M.F, muscle fibers; N, nuclei; F, inflammatory cells and B, blood engorged. A, G1 (control); B, G2 (TCVE); C, G3 ($HgCl_2$) and D, G4 ($HgCl_2$+TCVE). (MT, 400X).

changes in the myocardium (Figure 12D). The Masson's trichrome stain differentially colors healthy muscle fibers red, while fibrotic regions appear blue due to the accumulation of collagen

DISSCUSION

The study highlights the significant toxic effects of mercuric chloride ($HgCl_2$), a potent environmental pollutant, and the potential protective role of *Turbo cornutus* visceral extract (TCVE) against these effects. $HgCl_2$ exposure is known to adversely impact various biological systems, leading to detrimental alterations in growth rates, blood parameters, and histopathological changes in organs. This highly toxic form of mercury is present in various environments, such as air, water, and soil, and can result in kidney failure and digestive issues. Nevertheless, studies have indicated that the *Turbo cornutus* visceral extract utilization may mitigate the toxic effects of $HgCl_2$. This extract has exhibited anti-inflammatory properties and has been shown to decrease the production of nitric oxide and prostaglandin (Kim *et al*., 2022). Mercuric chloride leads to a decrease in the body weight of male albino rats, which is considered a significant indicator of rat health. These results are align with data obtained by Uzunhisarcikli *et al*. (2016). In parallel, our findings are consistent with Necib *et al*. (2013), who observed a decrease in rat weights due to mercuric chloride exposure. Exposure to $HgCl_2$ resulted in various chromosomal abnormalities that were not present in the control or TCEV groups, including fragments, breaks, ring chromosomes, and fractions in the G3 and G4. The data obtained in this study aligns with the results of Boujbiha *et al*. (2012), who also observed multiple types of chromosomal aberrations caused by mercuric chloride

Biochemical analysis of blood of the four experimental rats, focusing on LDH, glucose, protein, and CK levels, which serve as important indicators of various pathological conditions, showed significant variation among the groups. Our findings revealed that LDH levels were elevated in the G3 ($HgCl_2$) group, indicating liver damage caused by mercury poisoning, consistent with previous studies (Jagaadesan and Bharathi, 2014). Meanwhile, CK levels, used to assess heart and brain damage, were also increased in rats injected with $HgCl_2$ but decreased in the TCVE and $HgCl_2$-treated group compared to the $HgCl_2$-poisoned group (EL-Sawi *et al*., 2017). This result prove the protective effect of TCVE which compensate the damage effect of $HgCl_2$. Blood glucose levels were also measured, revealing significantly higher levels in the G3 ($HgCl_2$) group, consistent with data obtained by Setiyowati *et al*. (2019), which reported that exposure to mercury can lead to hyperglycemia and impaired glucose metabolism. The TCVE treatment helped reduce glucose levels compared to the poisoned group. Total protein levels, which indicate liver function, were found to be lowest in the G3 ($HgCl_2$) group, suggesting liver dysfunction. However, the TCVE treatment improved the protein levels in the G4 ($HgCl_2$+TCVE) group compared to the G3 ($HgCl_2$) group, consistent with the findings of EL-Demerdash (2001).

Histopathological analysis revealed critical insights into the organ-specific damage caused by $HgCl_2$. The observed Kupffer cell enlargement in the liver, renal tubular damage, and heart edema in the $HgCl_2$-exposed group underscore the severity of mercury toxicity. These findings are corroborated by prior studies that have documented similar pathological changes in response to mercury exposure (Theissen *et al.*, 2024). Histopathological examinations using H&E staining revealed liver abnormalities such as central vein dilation and sinusoidal space dilation, consistent with previous studies by Goudarzi *et al.* (2017); Uzunhisarcikli *et al.* (2016); Karuppanan *et al*. (2014); and Miah (2012). $HgCl_2$ led to endothelial debilitation in renal tubules, glomerular decay, and hyaline casts, aligning with findings from Miah (2021), Yadav *et al*. (2019), Youcef *et al*. (2013), and Al-Madani *et al*. (2009). The heart exhibited muscle filament alterations, nucleus necrosis, and striation breakdown, consistent with Karaboduk *et al.* (2015); Vijayakumar *et al*. (2014); and Azevedo *et al*. (2011). Masson's trichrome stain highlighted collagen filament differences among the groups, showing thick fibrous septa, collagen filaments, and bile duct accumulation in the liver. Additionally, fibrous casts increased in renal glomeruli in the G3 ($HgCl_2$), in line with Nabil *et al*. (2020). Furthermore, fibrous deposits in the heart of G4 ($HgCl_2$+TCVE) were enhanced. The administration of TCVE in the $HgCl_2$ + TCVE-treated group (G4) showed a marked reduction in the severity of these pathological changes, indicating that the antioxidants present in the extract may play a crucial role in preserving organ integrity and function. This protective effect aligns with the growing body of evidence supporting the use of natural antioxidants in mitigating heavy metal toxicity. In addition, the results of this study suggest that TCVE has the potential to counteract the toxic effects of mercuric chloride, enhancing growth rates and maintaining biochemical homeostasis. However, further research is warranted to elucidate the specific mechanisms through which TCVE exerts its protective effects and to explore its therapeutic applications in managing heavy metal toxicity. Understanding these mechanisms could cover the way for developing effective treatments for mercury poisoning and other related environmental health issues.

CONCLUSION

Evaluation the data obtained in this study, it was evident that mercuric chloride had detrimental effects and was toxic to the organs and variables under investigation. Over a period of five weeks, rats exposed to mercuric chloride exhibited a decrease in body weight, while those treated with *T. cornutus* showed improved growth and survival rates. Exposure to $HgCl_2$ also resulted in chromosomal abnormalities, including deletions, rings, breaks, and fragments. Furthermore, the presence of mercuric chloride led to increased levels of lactate dehydrogenase (LDH), creatine kinase (CK), and glucose, along with a decrease in total protein levels. In contrast, rats treated with TCVE extract demonstrated stability and improvement in these biochemical parameters. Histological and histochemical analyses of the liver, kidney, and heart revealed pathological changes induced by mercuric chloride. The use of TCVE extract showed promise in enhancing growth rates, maintaining chromosomal integrity, improving biochemical parameters, and mitigating histopathological and histochemical alterations.

REFERENCES

ABD EL-AZIZ, Y.M., H.K. ZAKY, A.E. KHALAF, M.K. HUSSIEN, N.G. SALAH, A.A. MAHMOUD, H.M. ELDEMERY, AND A.H. ABU-ALMAATY 2022. Evaluation of toxicity effects on tissues of kidney, heart, and chromosomes *in vivo* induced by sodium bicarbonate and the possible treatment by ethanolic extract solid dried tubers for *Cyperus esculentus*. Alfarama journal of basic and applied sciences. https://doi.org/10.2160-8/ajbas.2022.147844.1111.

ABDEL-MISIH, S.R., AND M. BLOOMSTON 2010. Liver Anatomy. Surgical Clinics, 90(4): 643-653.

ABU ALMAATY, A.H.A., B.M. HENDAM, F. ALTHOBAITI, E. FAYAD, AND Y.M. ABD EL-AZIZ 2022. Evaluation of the hepatoprotective and antioxidant effects of *Tegillarca granosa* flesh body extract against potassium bromide toxicity via targeting the histomorphometry, chromosomal and expressions of TGF-B1, VEGF and COX-2 genes in rats. Biocell, 46(1): 219. Doi: https://doi.org/1-0.32604/biocell.2022.017623.

AL-MADANI, W.A., N.J. SIDDIQI, AND A.S. ALHOMIDA 2009. Renal toxicity of mercuric chloride at different time intervals in rats. Biochemistry Insights, 2, BCI-S2928. Doi: https://doi.org/10.4137/BCI.S2928.

ALMATRAFI, M. Evaluating the renal and splenic protective effects of grape seed proanthocyanidin extract in diethylnitrosamine-induced male Sprague Dawle. Catrina: The International Journal of Environmental Sciences, 2024; 30(1): 41-49. doi: 10.21608/cat.2024.283071.1273

ARACKAL, A., AND K. ALSAYOURI 2019. Histology, heart.

AZEVEDO, B.F., H.D.A.F. NETO, I. STEFANON, AND D.V. VASSALLO 2011. Acute cardiorespiratory effects of intracisternal injections of mercuric chloride. neurotoxicology, 32(3): 350-354. Doi: https://doi.org/10.1016/j.neuro.20-11.02.006.

BOUJBIHA, M.A., G. BEN SALAH, A. BEN FELEH, M. SAOUDI, H. KAMOUN, A. BOUSSLEMA, AND A. EL FEKI 2012. Hematotoxicity and genotoxicity of mercuric chloride following subchronic exposure through drinking water in male rats. Biological trace element research, 148: 76-82.

BOUJBIHA, M.A., K. HAMDEN, F. GUERMAZI, A. BOUSLAMA, A. OMEZZINE, A. KAMMOUN,

AND A. EL FEKI 2009. Testicular toxicity in mercuric chloride treated rats: Association with oxidative stress. Reproductive toxicology, 28(1): 81-89. Doi: https://doi.org/10.1016/j.reprotox.2009.03.011.

CUNHA, I., A.C. SAWAYA, F.M. CAETANO, M.T. SHIMIZU, M.C. MARCUCCI, F.T. DREZZA, AND P.D.O. CARVALHO 2004. Factors that influence the yield and composition of Brazilian propolis extracts. Journal of the Brazilian Chemical Society, 15: Z 964-970. Doi: https://doi.org/10.1590/S0103-50532004000600026.

EL-DEMERDASH, F.M. 2001. Effects of selenium and mercury on the enzymatic activities and lipid peroxidation in brain, liver, and blood of rats. Journal of Environmental Science and Health, Part B, 36(4): 489-499. Doi: 10.1081/PFC-100104191.

EL-SAWI, M., M. AMER, AND S. MUFTAH 2017. Thymoquinone protects against mercuric chloride-induced hepatorenal toxicity in male rats. Journal of Agricultural Chemistry and Biotechnology, 8(1): 9-14. Doi:

EZEUKO, V.C., C.R. NWOKOCHA, P.E. MOUNMBEGNA, AND C.C. NRIAGU 2007. Effects of *Zingiber officinale* on liver function of mercuric chloride-induced hepatotoxicity in adult wistar rats. Electron J Biomed., 3: 40-45. Doi: https://www.researchgate.net/publication/200124588.

FISCHER, A.H., K.A. JACOBSON, J. ROSE, AND R. ZELLER 2008. Hematoxylin and eosin staining of tissue and cell sections. Cold Spring Harbor Protocols, (5), Doi: 10.1101\pdp.prot4986.

FRANCIS, M.Y., B. KARUNAKARAN, F. ASHFAQ, Y.M. QATTAN, I. AHMAD, A.G. ALKHATHAMI, AND P.S. KASIRAJAN 2023. Mercuric chloride induced nephrotoxicity: Ameliorative effect of *Carica papaya* leaves confirmed by histopathology, immunohistochemistry, and gene expression studies. ACS omega, 8(24): 21696-21708. Doi: https://doi.org/10.1021/acsomega.3c01045.

GOUDARZI, M., M. KALANTAR, AND H. KALANTAR 2017. The hepatoprotective effect of gallic acid on mercuric chloride-induced liver damage in rats. Jundishapur Journal of Natural Pharmaceutical Products, 12(4). Doi: https://doi.org/10.5812/jjnpp.12345.

HUANG, Y.L., S.L. CHENG, AND T.H. LIN 1996. Lipid peroxidation in rats administrated with mercuric chloride. Biological Trace Element Research, 52: 193-206.

JAGADEESAN, G., AND E. BHARATHI 2014. *In vivo* Restoration of hepatic and nephro protective potential of hesperidin and ellagic acid against mercuric chloride intoxicated rats. Biomedicine & Aging Pathology, 4(3): 219-222. Doi: https://doi.org/10.1016/j.biomag.2014.01.008.

KARABODUK, H., M. UZUNHISARCIKLI, AND Y. KALENDER 2015. Protective effects of sodium selenite and vitamin e on mercuric chloride-induced cardiotoxicity in male rats. Brazilian Archives of Biology and Technology, 58: 229-238. Doi : https://doi.org/10.1590/S1516-8913201400339.

KARUPPANAN, M., M., KRISHNAN, P. PADARTHI, AND E. NAMASIVAYAM 2014. Hepatoprotective and antioxidant effect of *Mangifera indica* leaf extracts against mercuric chloride-induced liver toxicity in mice.Euroasian journal of hepato-gastroenterology, 4(1). Doi:10.5005/jp-journals-10018-1091.

KIM, E.A., N., KANG, J., KIM, H.W., YANG, G. AHN, AND S.J. HEO 2022. Anti-inflammatory effect of *Turbo cornutus* viscera methanolic extract against lipopolysaccharide-stimulated inflammatory response via the regulation of the JNK/NF-Kb signaling pathway in murine macrophage RAW 264.7 cells and a zebrafish model: a preliminary study. Foods, 11(3): 364. Doi: https://doi.org/10.3390/foods11030364.

KING, L., AND G. WEBER 1986. Conformational drift of dissociated lactate dehydrogenases. Biochemistry, 25(12): 3632-3637.

Kim, Eun-A, Nalae Kang, Junseong Kim, Hye-Won Yang, Ginnae Ahn, and Soo-Jin Heo. 2022. "Anti-Inflammatory Effect of Turbo cornutus Viscera Ethanolic Extract against Lipopolysaccharide-Stimulated Inflammatory Response via the Regulation of the JNK/NF-kB Signaling Pathway in Murine Macrophage

KRISHNA, M. 2013. Role of special stains in diagnostic liver pathology. Clinical Liver Disease, 2, S8-S10. Doi: 10.1002/cld.148.

MADRAZO-IBARRA, A., AND P. VAITLA, 2023. Histology, Nephron. in StatPearls Publishing.

MCMILLIN, J.M. 1990. Blood glucose. in: Walker HK, Hall WD, Hurst JW, editors. Clinical Methods: The History, Physical, and Laboratory Examinations. 3rd ed. Boston: Butterworths. Chapter 141.

MIAH, M.A. 2021. Deleterious effects of mercuric chloride on blood biochemistry, liver and kidney histology in female albino mice. Journal of Agriculture, Food and Environment, 2(2) : 18-23. Doi: https://doi.org/10.47440/JAFE.2021.2204.

NABIL, A., M.M., ELSHEMY, M. ASEM, AND H.F. GOMAA 2020. Protective effect of DPPD on mercury chloride-induced hepatorenal toxicity in rats. journal of toxicology, 7. Doi: http://doi.org/1155/2020/4127284.

NECIB, Y., A. BAHI, AND S. ZERIZER 2013. Argan oil (*Argania spinosa l*) provides protection against mercuric chloride induced oxidative stress in rat albinos wistar. Int J Bas Applied Sci., 2: 73-80. Doi: 10.14419/ijbas.v2i1.540.

NORMAN, H., A. PAUL, AND D. MARLENE 1977. Purification of mitochondrial creatine kinase: two interconvertible forms of the active enzyme. Biocem. Biophys. Res. Commun., 79(3): 950-956. Doi: 10.1016/0006-291x(77)91594-7.

ORIQUAT, G.A., T.H. SALEEM, AND R.R. NAIK 2012. A sub-chronic toxicity study of mercuric

chloride in the rat. Jordan Journal of Biological Sciences, 5(2): 141-146.

PARAMJIT GROVER, B.SALEHA BANU, K.DANA DEVI, SAYEEDA BEGUM. 2001. *In vivo* genotoxic effects of mercuric chloride in rat peripheral blood leucocytes using comet assay, Toxicology, 167 (3): 191-197.

SAITO, H., AND H. AONO 2014. Characteristics of lipid and fatty acid of marine gastropod *Turbo cornutus*: High levels of arachidonic and N-3 docosapentaenoic acid. Food Chemistry, 145: 135-144. Doi: https://doi.org/10.1016/j.foodchem.2013.08.011.

SETIYOWATI, I., H. SUPRAPTO, AND G. MAHASRI 2019. The effects of mercury chloride ($HgCl_2$) on the changes in hematology and blood sugar level in carps (*Cyprinus carpio*). In IOP Conference Series: Earth and Environmental Science. 236(1). Doi: 10.1088/1755-1315/236/1/012104.

SIBULESKY, L. 2013. Normal liver anatomy. Clinical liver disease., 2: S1-S3. Doi: 10.1002/cld.124.

SINGH, P., AND V. SANKHLA 2010. *In situ* protective effect of curcumin on cadmium chloride induced genotoxicity in bone marrow chromosomes of swiss albino mice. Journal of Cell & Molecular Biology, 8(2).

THEISSEN, K., D. WEIL, AND J. GIFT. Summary Review Of Health Effects Associated With Mercuric Chloride: Health Issue Assessment. U.S. Environmental Protection Agency, Washington, D.C., EPA/600/R-92/199 (NTIS PB95201745).

UZUNHISARCIKLI, M., A. ASLANTURK, S. KALENDER, F.G. APAYDIN, AND H. BAS, 2016. Mercuric chloride induced hepatotoxic and hematologic changes in rats: The protective effects of sodium selenite and vitamin E. Toxicology and Industrial Health, 32(9): 1651-1662. Doi: https://doi.org/10.1177/0748233715572561.

VIJAYAKUMAR, M., G. JAGADEESAN, AND E. BHARATHI, 2014. Protective role of *Terminalia arjuna* seed extract formulations against cardiotoxicity induced by mercuric chloride in wister rats. Int. J. Pharmac. & Biol. Arch., 5: 158-165.

WATERBORG, J.H. 2009. The Lowry Method for Protein Quantitation. The protein protocols handbook.7-10.

YADAV, H.N., U.S. SHARMA, S. SINGH, AND Y.K. GUPTA 2019. Effect of *Tribulus terrestris* in mercuric chloride-induced renal accumulation of mercury and nephrotoxicity in rat. Journal of Advanced Pharmaceutical Technology & Research, ,10(3): 132-137. Doi:10.4103/japtr.JAPTR_386_18.

YOUCEF, N., B. AHLEM, AND Z. SAKINA 2013. Protective role of sodium selenite on mercuric chloride induced oxidative and renal stress in rats.Journal of Stress Physiology & Biochemistry, 9(2): 159-172.

التأثيرات الوقائية لمستخلص القوقع الحلزوني المقرنة ضد التغيرات المرضية الناجمة عن $HgCl_2$ في أنسجة الفئران البيضاء

ياسمين عبدالعزيز، ميرنا كذلك، ندى فاروق، مريم حلمى، ايه محمد، نورا عوض، رنا حامد، على ابوالمعاطى

قسم علم الحيوان، كلية العلوم، جامعة بورسعيـد، بورسعيـد، جمهورية مصر العربية

الملخص العربـــي

يعتبر كلوريد الزئبق هو مركب سام من ملح الزئبق وملوث ضار موجود في اماكن محتـلفة، ويصل للإنسان من أكل الأسماك والمأكولات البحرية الملوثة. و تناولت هذه الدراسة تأثير كلوريد الزئبق على معدل نمو الجرذان وتغيرات في الكروموسومات وقياسات الدم والفحوصات النسيجية المرضية لبعض الأعضاء، وقد استخدمنا مستخلص القوقع الحلزوني *Turbus cornutus* وهو حلزون بحري يتكون من مضادات الأكسدة ويمكن الحصول عليه بسهولة من البحر لعلاج الآثار الضارة الناجمة عن كلوريد الزئبق. تمت الدراسة على عدد أربعون من ذكور الجرذان وتوزيعهم عشوائيًا على أربع مجموعات (10 جرذان/ 2 ففص)؛ المجموعة الأولى هي المجموعة الضابطة، والمجموعة الثانية تناولت 200 ملجم/كجم من مستخلص القوقع، وتعرضت المجموعة الثالثة لـ 20/1 من نصف الجرعة المميتة من كلوريد الزئبق، وكانت المجموعة الرابعة مجموعة معرضة لكلوريد الزئبق بالإضافة إلى مستخلص القوقع كمثل الجرعات في المجموعتين الثانية والثالثة. وبعد خمس أسابيع من التغذية والعلاج قمنا بالذبح الرحيم للجرذان وتم تسجيل النتائج. أظهرت الجرذان المعاملة بمستخلص القوقع ثباتًا في قياساتها مقارنة بالمجموعة الأولى. أما بالنسبة للمجموعة الثالثة التي تعرضت لكلوريد الزئبق أدت لتغيرات في معدل النمو، ومعايير الدم، وكذلك تغيرات مرضية نسيجية مثل تضخم خلايا كوبفر في الكبد، وتلف بالأنابيب الكلوية، وذمة بعضلات القلب. أما المجموعة الرابعة أظهرت تحسن ملحوظ على مستوى معدل نمو الجرذان والكروموسومات وقياسات الدم والفحوصات النسيجية المرضية لأعضاء الكبد والكلى وعضلات القلب.